

Discrete Analog of the Burgers Equation

E. Ben-Naim¹ and P. L. Krapivsky²

¹*Theoretical Division and Center for Nonlinear Studies,
Los Alamos National Laboratory, Los Alamos, NM 87545, USA*
²*Department of Physics, Boston University, Boston, MA 02215, USA*

We propose the set of coupled ordinary differential equations $dn_j/dt = n_{j-1}^2 - n_j^2$ as a discrete analog of the classic Burgers equation. We focus on traveling waves and triangular waves, and find that these special solutions of the discrete system capture major features of their continuous counterpart. In particular, the propagation velocity of a traveling wave and the shape of a triangular wave match the continuous behavior. However, there are some subtle differences. For traveling waves, the propagating front can be extremely sharp as it exhibits double exponential decay. For triangular waves, there is an unexpected logarithmic shift in the location of the front. We establish these results using asymptotic analysis, heuristic arguments, and direct numerical integration.

PACS numbers: 05.45.-a, 02.60.-Lj, 02.50.-r

The classic Burgers equation

$$n_t + (n^2)_x = \nu n_{xx} \quad (1)$$

is the simplest partial differential equation which incorporates both nonlinear advection and diffusive spreading [1–6]. This ubiquitous equation emerges naturally in the presence of dissipation, and it is broadly used to model traffic flows [2], transport processes [7, 8], surface growth [9, 10], and large scale formation of matter in the Universe [11, 12].

The Burgers equation has two important properties. The first is continuity: equation (1) can be written in the form $n_t + J_x = 0$, hence assuring mass conservation in the absence of sources or sinks. If we view the quantity n as a density, then the total mass is a conserved quantity, $\int_{-\infty}^{\infty} dx n(x, t) = \text{const.}$, as long as the density vanishes, $n(x) \rightarrow 0$ in the limits $x \rightarrow \pm\infty$. The second property is asymmetry: due to the nonlinear advection term, equation (1) is not invariant with respect to the inversion transformation $x \rightarrow -x$.

Our goal is to construct a discrete (in space) counterpart of the Burgers equation that maintains these two properties [13–16]. Thus we discretize the spatial coordinate but keep the time variable continuous, $n(x, t) \rightarrow n_j(t)$, where j is integer. The differential equation

$$\frac{dn_j}{dt} = f(n_{j-1}) - f(n_j) \quad (2)$$

represents a continuity equation on a one-dimensional lattice. Indeed, a finite total mass $M = \sum_{j=-\infty}^{\infty} n_j$ remains constant, $M = \text{const.}$, if two conditions are met: (i) a vanishing density $n_j \rightarrow 0$ as $j \rightarrow \pm\infty$, and (ii) a vanishing function f at the origin, $f(0) = 0$. To reproduce the nonlinear advection term in (1), we take a purely quadratic and positive function $f(n) = n^2$. With this choice, we arrive at the set of nonlinear difference-differential equations

$$\frac{dn_j}{dt} = n_{j-1}^2 - n_j^2. \quad (3)$$

This system of equations meets the two criteria of mass conservation and asymmetry.

Immediately, we can point out an important difference between the discrete equation (3) and the continuous equation (1). Let us treat the spatial variable in (3) as continuous, $j \rightarrow x$, and replace the difference with a second order Taylor expansion. The result of these two steps is the continuous equation

$$n_t + (n^2)_x = (nn_x)_x. \quad (4)$$

By construction, the nonlinear advection term is the same as in (1). However, the viscosity equals the density, $\nu = n$, whereas in the original Burgers equation, the viscosity is constant. We restrict our attention to positive densities,

$$n > 0, \quad (5)$$

so that the solutions of (3) are stable (avoiding a negative diffusion instability). We note that transport coefficients often depend on density or temperature; in fluid dynamics [4, 5], for example, transport coefficients vary as \sqrt{T} for hard-sphere gases.

Equation (3) describes the evolution of the probability density in a two-body analog of the standard Poisson process [17]. For example, we mention a homophilic network growth process [18]. In the canonical random network model, a pair of nodes are chosen at random and subsequently, the two are connected by a link. This elementary step is repeated indefinitely, and in finite time, a percolating network emerges. As a model of homophilic networks where only similar entities interact, we considered the situation where only nodes with exactly the same degree can be connected [19]. The degree distribution $n_j(t)$, that is, the fraction of nodes of degree j at time t , obeys the rate equation (3). The initial condition $n_j(0) = \delta_{j,0}$ represents a disconnected set of nodes. In this network context, the quantity $n_j(t)$ is a probability density, and mass conservation guarantees proper normalization, $\sum_{j=0}^{\infty} n_j = 1$. Moreover, the condition (5) reflects that probability distribution functions are by definition positive.

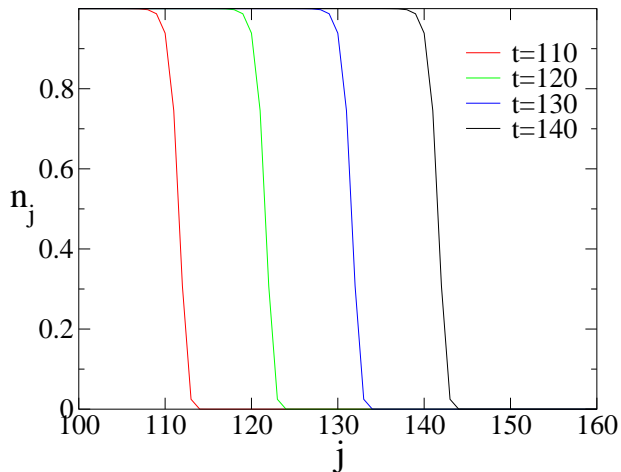


FIG. 1: The traveling wave. Shown is the function $n_j(t)$ versus j at four different times: $t = 110, 120, 130, 140$. The results are from numerical integration of the Eq. (3) subject to the step initial condition (6).

In this paper, we discuss the solutions of the discrete equation (3) in view of the well known solutions of the continuous equation (1). Using a combination of theoretical and numerical methods, we analyzed the solutions of the discrete equation for the following standard initial conditions [2]: (i) a step function resulting in a traveling wave, (ii) a localized delta function leading to a triangular wave, and (iii) a complementary step function with an ensuing rarefaction wave. For all of these cases, we find that the discrete analog faithfully captures the primary features of the continuous Burgers equation. However, we also find subtle and interesting departures from the classical solutions in the first two cases. Therefore, in the rest of this paper, we focus on traveling waves (also known as shock waves) and triangular waves.

Traveling Waves

We first consider the step function initial condition

$$n_j(0) = \begin{cases} 1 & j \leq 0 \\ 0 & j > 0. \end{cases} \quad (6)$$

Using the convenient Adams-Bashforth method [20, 21], we numerically integrate the rate equation (3) and find that the solution approaches a traveling wave (figure 1)

$$n_j(t) \rightarrow G(j - vt), \quad (7)$$

in the long-time limit. The function $G(z)$ specifies the form of the traveling wave and v is the propagation velocity. Of course, the function $G(z)$ has the limiting behaviors $\lim_{z \rightarrow -\infty} G(z) = 1$ and $\lim_{z \rightarrow \infty} G(z) = 0$.

To find the propagation velocity, we first note that according to equations (3) and (6), the density does not evolve, $n_j(t) = 1$ when $j \leq 0$. Next, we define the mass

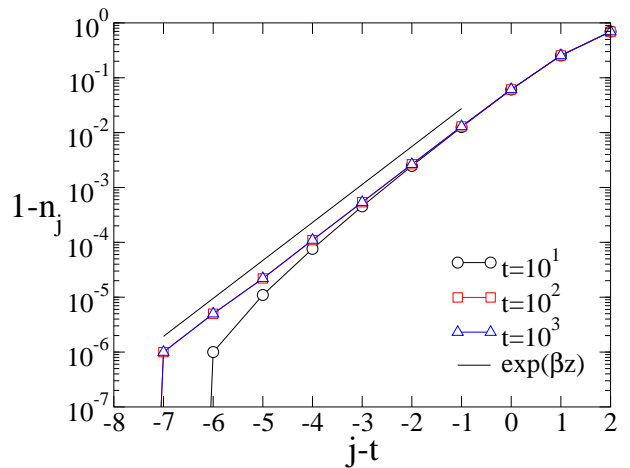


FIG. 2: The negative- z tail of the function $G(z)$. Shown is the quantity $1 - n_j$ versus $j - t$ at various times. The theoretical prediction (12) with $\beta = 1.59362$ is also shown for reference.

in the positive half space, $M_+(t) = \sum_{j=1}^{\infty} n_j(t)$, and note that summation of (3) gives

$$\frac{dM_+}{dt} = n_0^2. \quad (8)$$

Since $M_+(0) = 0$ and $n_0(t) = 1$, the mass equals time, $M_+ = t$. This fact, along with equation (7) and the limiting behaviors of the function $G(z)$, gives the velocity

$$v = 1. \quad (9)$$

Hence, the propagation velocity, which is dictated by mass conservation, agrees with the continuous value [22].

To characterize the shape of the traveling wave, we substitute the form (7) into the governing equation (3). The function $G(z)$ satisfies the nonlinear and nonlocal differential equation

$$G'(z) = G^2(z) - G^2(z - 1), \quad (10)$$

where prime denotes derivative with respect to z . We now use asymptotic analysis to obtain the leading asymptotic behaviors of $G(z)$ in the limits $z \rightarrow \pm\infty$.

Since $G(z) \rightarrow 1$ when $z \rightarrow -\infty$, we substitute $G(z) = 1 - \phi(z)$ into equation (10), and obtain a *linear* yet nonlocal equation for the correction function ϕ ,

$$\phi'(z) = 2[\phi(z) - \phi(z - 1)]. \quad (11)$$

Therefore, the correction decays exponentially, $\phi(z) \sim e^{\beta z}$. By substituting this behavior into (11), we find the decay constant $\beta = 1.59362$ as the nontrivial root of the transcendental equation $\beta = 2(1 - e^{-\beta})$. As shown in figure 2, the numerical results confirm that

$$1 - G(z) \sim e^{\beta z} \quad (12)$$

when $z \rightarrow -\infty$. This exponential behavior agrees, at least qualitatively, with the corresponding behavior in the continuous case [23].

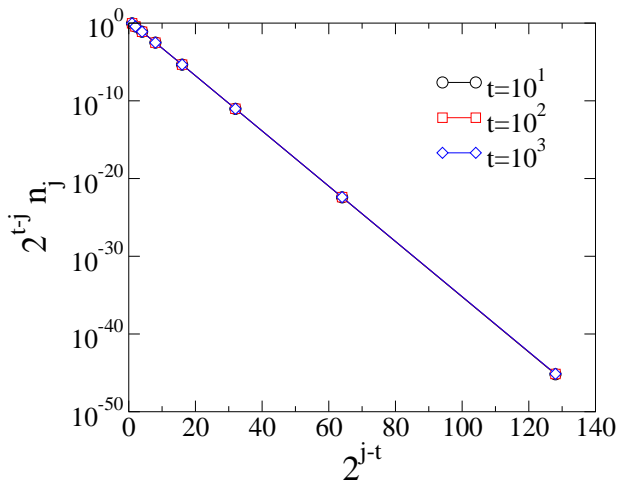


FIG. 3: The positive- z tail of the traveling wave function $G(z)$. Shown is $2^{j-t}n_j$ versus 2^{j-t} at three different times.

In the complimentary $z \rightarrow \infty$ limit, we expect that $G(z) \rightarrow 0$. Now, the positive term in (10) is negligible, and the behavior is governed by the *nonlinear* and non-local equation $G'(z) = -G^2(z-1)$. We use the WKB transformation [24] $G(z) \simeq \Psi \exp(-\psi)$ and arrive at the linear relation

$$\psi(z) = 2\psi(z-1). \quad (13)$$

We thus obtain the exponential solution $\psi(z) = \gamma 2^z$ and further, the prefactor $\Psi(z) = (4 \ln 2)\psi(z)$. The constant γ cannot be determined in the realm of asymptotic analysis; numerically, we obtain $\gamma = 0.818$. Remarkably, the leading tail of the traveling wave is extremely sharp, as it follows the unusual double exponential decay (figure 3)

$$G(z) \sim 2^z e^{-\gamma 2^z} \quad (14)$$

when $z \rightarrow \infty$. Hence, the front of the propagating wave does not extend beyond a few lattice sites (see figure 1). In the continuous case the traveling wave is specified by $G_{\text{cont}}(z) = \frac{1}{2}[1 - \tanh(z/2\nu)]$ and hence, the shape is symmetric as $G_{\text{cont}}(z) + G_{\text{cont}}(-z) = 1$. Therefore, the behavior in the discrete case differs in two ways. First, the shape of the traveling wave is asymmetric. Second, the leading tail of the wave follows a double-exponential decay, in contrast with the simple exponential decay in the continuous case.

To gain further insight into the extremely sharp front (14), we also study the continuous equation (4). We assume that the solution approaches a traveling wave, $n(x,t) \rightarrow g(x-vt)$, with velocity $v = 1$ (again, the velocity is set by the continuity condition). From Eq. (4), the function $g(z)$ obeys the ordinary differential equation

$$g' - 2gg' + (gg')' = 0. \quad (15)$$

Integration of this equation is immediate, and using the limiting behavior $g \rightarrow 0$ as $z \rightarrow \infty$, we have $g' = g - 1$.

We now invoke the limiting behavior $g \rightarrow 1$ as $z \rightarrow -\infty$ and find

$$g(z) = \begin{cases} 1 - e^{z-z_0} & z \leq z_0, \\ 0 & z \geq z_0. \end{cases} \quad (16)$$

This family of solutions is parameterized by z_0 , a quantity that depends on the details of the initial conditions. Hence, the traveling wave is exponential *everywhere* behind the front which is located at $t + z_0$. In particular, the negative- z tail is analogous to (12). Remarkably, the leading front of the traveling wave is perfectly sharp [25–27] as the function g vanishes beyond the front location!

We view the double exponential decay (14) as a discrete analog of a perfectly sharp front. Moreover, the effective viscosity $\nu \equiv n$ and the vanishing density ahead of the propagating front are together responsible for the extremely sharp front [22].

Triangular Waves

Under the Burgers equation (1), an initial condition with compact support necessarily evolves into a triangular wave. Moreover, the shape of the triangular wave is universal. Without loss of generality, we consider the localized initial condition

$$n_j(0) = \delta_{j,1}. \quad (17)$$

As discussed above, according to the discrete equation (3), the total mass is conserved. Moreover, there is no evolution in the negative half-space, $n_j(t) = 0$ for $j \leq 0$. Therefore, the mass in the positive half space equals unity, $M_+(t) = \sum_{j \geq 1} n_j(t) = 1$.

Numerically, we integrate the discrete equation (3) starting with the initial condition (17) and find that the density adheres to the scaling form (figure 4)

$$n_j(t) \simeq \frac{1}{\sqrt{t}} F\left(\frac{j}{\sqrt{t}}\right). \quad (18)$$

Further, the scaling function is triangular (figure 4)

$$F(x) = \begin{cases} 0 & x < 0; \\ \frac{x}{2} & 0 < x < 2; \\ 0 & x > 2. \end{cases} \quad (19)$$

Therefore, the discrete equation (3) captures the basic features of the continuous equation (1).

The scaling behavior (18)–(19) follows from the inviscid Burgers equation $\partial n / \partial t + 2n \partial n / \partial j = 0$. Indeed, mass conservation, in conjunction with the inviscid Burgers equation, dictates the scaling form (18) and the normalization $\int_0^\infty dx F(x) = 1$. By substituting (18) into (1) and ignoring the diffusion term, we see that the function F obeys

$$\frac{d}{dx} \left[F \left(F - \frac{x}{2} \right) \right] = 0. \quad (20)$$

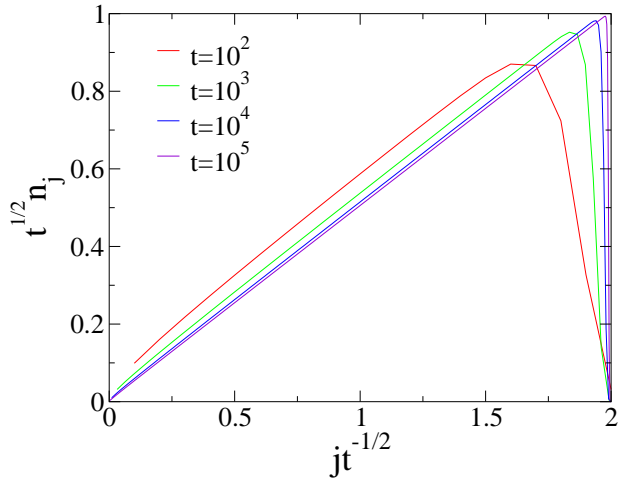


FIG. 4: The triangular wave. Shown is the function $t^{1/2}n_j(t)$ versus the scaling variable $jt^{-1/2}$ at different times.

There are two solutions, $F = x/2$ and $F = 0$, and consequently, the scaling function is piecewise-linear as in (19). Finally, the extent of the nonzero region, $0 < x < 2$, is set by the normalization condition.

We now analyze the solution of the discrete equation (3) in the asymptotic regime. The quantity n_1 satisfies the closed equation $dn_1/dt = -n_1^2$, and using the initial condition $n_1(0) = 1$, we have

$$n_1 = \frac{1}{1+t}. \quad (21)$$

This density is inversely proportional to time, $n_1 \simeq t^{-1}$ in the limit $t \rightarrow \infty$. The structure of the rate equations (3) suggests that in general, the densities n_j are inversely proportional to time,

$$n_j \simeq A_j t^{-1}, \quad (22)$$

when $t \rightarrow \infty$. Substitution of (22) into (3) shows that this asymptotic behavior is compatible with the rate equation, and furthermore, yields a quadratic recursion relation for the prefactors,

$$A_j^2 - A_j = A_{j-1}^2. \quad (23)$$

Starting with $A_1 = 1$, we can iteratively obtain the prefactors from the explicit formula

$$A_j = \frac{1 + \sqrt{1 + 4A_{j-1}^2}}{2} \quad (24)$$

leading to $A_2 = \frac{1+\sqrt{5}}{2}$, $A_3 = \frac{1+\sqrt{7+2\sqrt{5}}}{2}$, etc. [28].

We use a continuum approach to calculate the large- j asymptotic behavior of A_j . To obtain the leading asymptotic behavior, we convert equation (23) into the differential equation $dA/dj = 1/2$. Hence, to leading order, the coefficients are linear, $A_j \simeq j/2$, and from the asymptotic

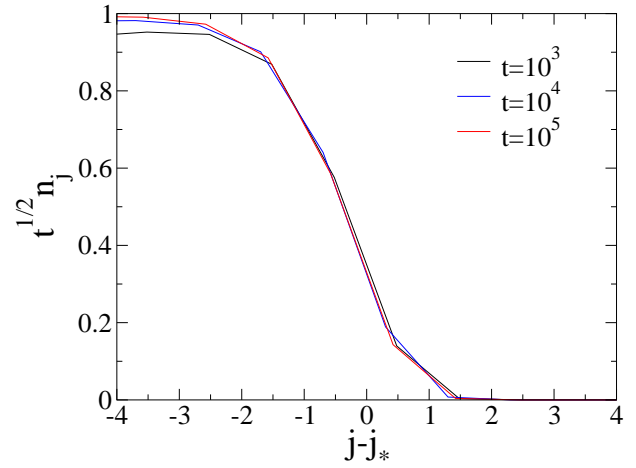


FIG. 5: The front of the triangular wave. Shown is the function $t^{1/2}n_j(t)$ versus $j - j_*$ with j_* given by (27) at different times.

behavior (22) one has $n_j \simeq j/(2t)$. We thus recover the continuous behavior indicated by (18) and $F(x) = x/2$.

There is, however, a correction to the leading asymptotic behavior. We substitute $A_j = j/2 + u_j$ into (23) and find that the correction u_j obeys the recursion

$$(j-1)(u_j - u_{j-1}) = \frac{1}{4} + u_{j-1}^2 - u_j^2, \quad (25)$$

and $u_1 = 1/2$. When j is large, the difference between the two quadratic terms is negligible, and the continuous approach gives $du/dj = 1/(4j)$. As a result, the prefactors include a logarithmic correction

$$A_j \simeq \frac{j}{2} + \frac{\ln j}{4} + C. \quad (26)$$

The constant $C = 0.32324$ is computed by numerical iteration of (24).

The logarithmic correction affects the location of the propagating wave. If we denote the front location by j_* , then mass conservation gives $\sum_{j=1}^{j_*} n_j \simeq 1$. Substitution of (22) and (26) into this sum yields

$$j_* \simeq 2\sqrt{t} - \frac{1}{4} \ln t, \quad (27)$$

by straightforward asymptotic analysis. The leading term follows from the continuous behaviors (18) and the extent of the triangular wave specified by (19). However, the logarithmic correction, which follows from the coefficient (26) constitutes a departure from the continuous behavior. We conclude that the triangular wave has the following form

$$n_j(t) \simeq \begin{cases} 0 & j \leq 0, \\ A_j t^{-1} & 0 < j \ll j_*, \\ 0 & j \gg j_*. \end{cases} \quad (28)$$

We already established the front location j_* and the maximal height of the wave $n_* \sim t^{-1/2}$ which follows

from (18) and (19). Thus, we anticipate the scaling behavior

$$n_j(t) \simeq \frac{1}{\sqrt{t}} G(j - j_*), \quad (29)$$

in the finite neighborhood $j - j_* \sim \mathcal{O}(1)$. Numerical integration confirms this scaling behavior (figure 5). The function $G(z)$ specifies the shape of the front. By substituting (29) and (27) into the rate equation (3), we see that the scaling function $G(z)$ satisfies (10). Hence, triangular waves and the traveling waves have identical fronts! This behavior is remarkable in view of the two very different scaling forms (18) and (29). In particular, the leading front is extremely sharp and follows the double exponential decay (14).

We also studied rarefaction waves by considering the complementary step function

$$n_j(0) = \begin{cases} 0 & j \leq 0, \\ 1 & j > 0. \end{cases} \quad (30)$$

Again, there is no evolution in the negative half space. According to the continuous equation (1), the density obeys the scaling behavior $n_j(t) \rightarrow F(j/t)$ with the very same $F(x)$ given by equation (19). Of course, there is a significant difference with the triangular wave as the extent of the wave is now linear in time. In addition, there are diffusive boundary layers, for example when $j - 2t \sim \mathcal{O}(t^{1/2})$. Numerical integration of the rate equation (3) shows that the scaling behavior and the diffusive boundary layer both agree with the continuous case.

In contrast with the traveling and triangular waves above, we can replace the difference equation (3) with the differential equation (1) even inside the front region because the size of the boundary layer grows diffusively with time. However, the discrete and the continuous equations are not equivalent when $j \sim \mathcal{O}(1)$ because of the vanishing viscosity.

Integrability is a remarkable feature of the Burgers equation: the Cole-Hopf transformation $n = -\nu u_x/u$ turns the nonlinear equation (1) into the ordinary diffusion equation $u_t = \nu u_{xx}$. Our discrete equation (3) is not integrable. Interestingly, however, the discrete equation

tion

$$\frac{dn_j}{dt} = n_j(n_j - n_{j-1}) \quad (31)$$

which has a purely quadratic right-hand-side and mimics the nonlinear advection term in the Burgers equation, can be linearized. The transformation [29]

$$n_j = \frac{q_j}{q_{j+1}} \quad (32)$$

reduces the nonlinear equation (31) into the linear equation $dq_j/dt = q_{j-1}$. Using this transformation, equation (31) can be solved exactly for the initial condition (30). From the solution $q_j = 1 + t + \frac{1}{2}t^2 + \dots + \frac{1}{(j-1)!}t^{j-1}$, the rarefaction wave discussed above follows immediately. However, the discrete equation (31) does not satisfy continuity. Constructing a discrete analog of the Burgers equation which satisfies the continuity condition, and in addition, can be transformed into a linear equation is an interesting challenge.

In summary, we introduced a discrete nonlinear equation that captures the key properties of the Burgers equation. Intriguingly, the most natural discrete analog of the Burgers equation is essentially unique: matching the nonlinear advection term dictates a viscosity that is equal to the density, $\nu = n$. The discrete equation satisfies the continuity condition and consequently, the mass of an initially localized ‘‘bump’’ is conserved. The mass conservation ensures that the velocity of a traveling wave and the shape of a triangular wave match the continuous behavior, to leading order. We also find that the shape of a triangular wave is identical to the continuous case.

In contrast with the classic Burgers equation, the viscosity equals the density. This discrepancy results in subtle departures from the continuous behavior: The shape of the traveling wave is asymmetric, and moreover, the front of the wave is extremely sharp with double exponential tail. Further, the front of the triangular wave includes a logarithmic-in-time correction to the leading behavior which is diffusive.

We gratefully acknowledge support for this research through DOE grant DE-AC52-06NA25396.

-
- [1] J. M. Burgers, *The Nonlinear Diffusion Equation*, (Springer, Berlin, 1974).
 - [2] G. B. Whitham, *Linear and Nonlinear Waves* (Wiley-Interscience, New York, 1974).
 - [3] J. D. Logan, *An introduction to Nonlinear Partial Differential Equations* (Hoboken, N.J., Wiley-Interscience, 2008).
 - [4] L. D. Landau and E. M. Lifshitz, *Fluid Mechanics* (Pergamon Press, New York, 1987).
 - [5] G. I. Barenblatt, *Scaling, Self-Similarity, and Intermediate Asymptotics* (Cambridge University Press, Cambridge, UK, 1996).
 - [6] P. L. Krapivsky, S. Redner and E. Ben-Naim, *A Kinetic View of Statistical Physics* (Cambridge University Press, Cambridge, UK, 2010).
 - [7] B. Schmittmann and R. K. P. Zia, Statistical Mechanics of Driven Diffusive Systems, in *Phase Transitions and Critical Phenomena*, Vol. 17, eds. C. Domb and J. L. Lebowitz (Academic Press, London)
 - [8] B. Derrida, Phys. Rept. **301**, 65 (1998).
 - [9] M. Kardar, G. Parisi, and Y. C. Zhang, Phys. Rev. Lett. **56**, 889 (1986).

- [10] A. -L. Barabasi and H. E. Stanley, *Fractal Concepts in Surface Growth* (Cambridge University Press, Cambridge 1995).
- [11] Ya. B. Zeldovich, *Astron. Astrophys.* **5**, 84 (1970).
- [12] S. F. Shandarin and Ya. B. Zeldovich, *Rev. Mod. Phys.* **61**, 185 (1989).
- [13] G. M. Henkin and V. M. Polterovich, *Jour. Nonlin. Sci.* **4**, 497 (1994); *Disc. Cont. Dynam. Sys.* **5**, 697 (1999).
- [14] K. Nishinari and D. Takahashi, *J. Phys. A* **31**, 5439 (1998).
- [15] R. Hernández Heredero, D. Levi, and P. Winternitz, *J. Phys. A* **32**, 2685 (1999).
- [16] Z. Artstein, C. W. Gear, I. G. Kevrekidid, M. Slermod, and E. S. Titi, *SIAM J. Num. Anal.* **49**, 2124 (2011).
- [17] For the standard Poisson process, $j \rightarrow j + 1$, the probability distribution function p_j obeys the rate equation $dp_j/dt = p_{j-1} - p_j$. Similarly, the rate equations (3) describe the evolution of the probability density for the “two-body” generalization $(j, j) \rightarrow (j + 1, j + 1)$.
- [18] M. E. J. Newman, *Networks: An Introduction* (Oxford University Press, Oxford 2010).
- [19] E. Ben-Naim and P. L. Krapisky, *J. Stat. Mech.* P11008 (2011).
- [20] F. Bashforth and J. C. Adams, *Theories of Capillary Action* (Cambridge University Press, London, 1883).
- [21] D. Zwillinger, *Handbook of Differential Equations* (Academic Press, London, 1989).
- [22] In general, propagation from the state $n = a$ into the state $n = b < a$ occurs with the velocity $v = a + b$ and the function $G(z)$ is always asymmetric. When $b > 0$, however, both tails of the function $G(z)$ are exponential.
- [23] Qualitatively, the exponential behavior is consistent with asymptotic behavior of the density $n_1 = \tanh t$.
- [24] C. M. Bender and S. A. Orszag, *Advanced Mathematical Methods for Scientists and Engineers* (McGraw-Hill, New York, 1978).
- [25] Ya. B. Zeldovich and A. S. Kompaneets, in: *Collection of Papers Dedicated to A. F. Ioffe*, pp. 61–71 (Izd. Akad. Nauk SSSR, Moscow, 1950).
- [26] G. I. Barenblatt, *Prikl. Mat. Mekh.* **16**, 67 (1952).
- [27] P. Rosenau and J. M. Hyman, *Phys. Rev. Lett.* **70**, 564 (1993).
- [28] When $j = 2$, the density n_j can be obtained analytically $n_2 = A_2 n_1 - (2A_2 - 1) [1 + t + (1 - A_2^{-1})(1 + t)^{2A_2}]^{-1}$.
- [29] E. Ben-Naim and S. Redner, *J. Stat. Mech.* L11002 (2005).